X-652-72-283

PREPRINT

DIELECTRIC CONSTANTS OF SOILS AT MICROWAVE FREQUENCIES

F. E. GEIGER
DONALD WILLIAMS

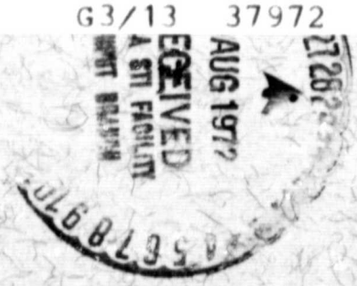

APRIL 1972

GODDARD SPACE FLIGHT CENTER
GREENBELT, MARYLAND

X-652-72-283

DIELECTRIC CONSTANTS OF SOILS AT MICROWAVE FREQUENCIES

F. E. Geiger and Donald Williams

April 1972

GODDARD SPACE FLIGHT CENTER
Greenbelt, Maryland

X-652-72-283

DIELECTRIC CONSTANTS OF SOILS AT MICROWAVE FREQUENCIES

F. E. Geiger and Donald Williams

April 1972

GODDARD SPACE FLIGHT CENTER
Greenbelt, Maryland

ABSTRACT

A knowledge of the complex dielectric constant of soils is essential in the interpretation of microwave airborne radiometer data of the Earth's surface. Measurements were made at 37 GHz on various soils from the Phoenix, Ariz., area. Extensive data have been obtained on $\epsilon = \epsilon' - j\epsilon''$ for dry soil and soil with water content in the range from 0.6 to 35 percent by dry weight. Measurements were made in a two-arm microwave bridge and results were corrected for reflections at the sample interfaces by solution of the parallel dielectric plate problem. The maximum dielectric constants are about a factor of 3 lower than those reported for similar soils at X-band frequencies.

CONTENTS

DIELECTRIC CONSTANTS OF SOILS AT MICROWAVE FREQUENCIES

F. E. Geiger and Donald Williams
Goddard Space Flight Center

INTRODUCTION

Purpose of Measurement

In the microwave region the emergent thermal radiation from a semi-infinite medium is proportional to the brightness temperature (by the Rayleigh-Jeans approximation, refs. 1 and 2)

$$T_b = (1 - |R_{12}|^2)\int_0^\infty \alpha(z)T(z)\exp\left[-\int_0^z \alpha(\xi)\,d\xi\right]dz \qquad (1)$$

where $|R_{12}|^2$ is the free-space power reflection coefficient of the semi-infinite medium 2 with respect to the medium 1 at the interface $z = 0$; $1 - |R_{12}|^2$ is the emissivity of medium 2, and is related to the thermodynamic temperature $T(z = 0)$ by $1 - |R_{12}|^2 = T_b/T(0)$; and $\alpha(z)$ is the free-space attenuation coefficient of the electromagnetic wave in medium 2 (not to be confused with the guide absorption constant α defined later); $|R_{12}|^2$ is related to the dielectric constant ϵ_2 of medium 2 by the Fresnel equations. Consequently, the emergent radiation becomes a direct function of the dielectric constant ϵ_2. But equation (1) also shows that T_b is a function of characteristics of the interior of medium 2. Radiometric measurements of thermal radiation are therefore dependent on a detailed knowledge of surface emissivities $(1 - R(\epsilon)^2$ and absorption constants $\alpha(z)$ and their dependence on physical conditions in the interior of the medium.

This paper reports on the determination of the complex dielectric constant $\epsilon = \epsilon' - j\epsilon''$ of a number of soil samples from the Phoenix, Ariz., area as a function of moisture content at a frequency of 37 GHz.

Review of Existing Methods

The experimental method for the measurement of ϵ must be suitable to measure the real part of the dielectric constant[1] in the range $2.5 < \epsilon'/\epsilon_0 < 10$ and the imaginary part from $0.05 < \epsilon''/\epsilon_0 < 10$.

[1]SI units are used throughout; $\epsilon_0 = 8.85 \times 10^{-12}$ F m^{-1}.

Four previously used methods were considered for these measurements:

(1) Transmission measurements between two points in an infinite line

(2) Input impedance measurements on a finite line

(3) Cavity resonance methods

(4) Free-space transmission measurements

A thorough discussion of the first two is given by Westphal (ref. 3), and specific examples of application of the first to water are given by Buchanan (ref. 4), to soils and water by Straiton and Tolbert (ref. 5), and to ice and snow by Cumming (ref. 6). The second method has been used by von Hippel (ref. 7) on a wide variety of materials, solid and liquid, and for a wide range of ϵ' and ϵ''.

Cylindrical cavity resonations have been used in the transverse magnetic (TM_{010}) and transverse electric (TE_{01n}) modes with disk- and rod-shaped samples. Solutions of Maxwell's equations for these various configurations and modes have been worked out by Horner et al. (ref. 8), and Tkach (ref. 9). Tkach measured a large variety of solids and liquids with relatively high ϵ' and ϵ'' ($\epsilon'/\epsilon_0 \sim 20$, $\epsilon''/\epsilon_0 \sim 2$).

Straiton and Tolbert (ref. 5) have used free-space transmission methods on both soil and water.

Choice of Methods

The suitability of the standing-wave detector for measuring a wide range of impedances and the elegance of von Hippel's method (ref. 7) makes the input impedance method very attractive. Serious drawbacks for accurate measurements would seem to be the apparent unavailability of commercial precision voltage standing-wave ratio (VSWR) bridges in the centimeter and millimeter ranges. Von Hippel's apparatus for a wavelength of $\lambda = 6$ cm had a probe position accuracy of 0.0025 cm (0.001 in.). Greatest sensitivity is achieved when the length of lossy sample is approximately an odd multiple of guide wavelengths (in the dielectric). For free-air wavelengths of 0.8 and 1.6 cm, optimum sample lengths are found to be on the order of 5 and 12 mm, respectively. For soil samples this probably would give unrepresentative results. Very lossy samples would be insensitive to the length of the sample because the sample impedance approaches the guide wave impedance.

In cylindrical cavity resonance methods at high frequencies, one has to contend with small cavities. TM modes have high axial electric fields and result in smaller cavities than do TE modes. The latter have no axial fields and may be suitable for relatively high loss measurements. Using Tkach's (ref. 9) equations for TE_{01n} modes and coaxial cylindrical samples, calculations show that for 19 and 37 GHz, and diameter to length of cavity ratios of $(D/L)^2 \sim 1/10$, sample diameters are less than 0.5 and 0.25 cm, respectively. This corresponds to an upper limit in the loss tangent of approximately $\tan \delta < 0.005$ for both frequencies. These figures show clearly that soil sample measurements are not practical in this

frequency range by cavity resonance methods. Considerations for 5 GHz show that specimens 1 cm in diameter could be used for tan $\delta \leq 0.01$.

Free-space transmission measurements have the advantage that sample preparation is very simple for high-loss samples. The sample can be placed on a plastic tray between two microwave horns of a bridge (ref. 10). For low-loss samples this may be impractical. Further, some factors in the measurements are difficult to assess, such as spherical wave fronts, horn antenna patterns with samples of different refractive index, and $1/r$ effects in large samples.

An elegant free-space ellipsometer method apparently was introduced by Pozdniak (ref. 11). Elliptically polarized radiation reflected from a surface can be analyzed in terms of the polarization coefficient. The polarization coefficient in turn is a function of the dielectric constant of the surface. However, radiation incident on a rough surface suffers depolarization changing the polarization coefficient (phase and amplitude). Hence this method probably has only limited applicability for soils.

The last method to be discussed is the transmission method on an infinite line, as suggested by T. Willeit (personal communication). Although it is a straightforward measurement of attenuation and phase, its accuracy is limited primarily by the calibration accuracy for attenuation and phase shift. It can, however, cover a wide range of ϵ' and ϵ'' with good accuracy, especially when used in a bridge configuration. It has the advantage that sample sizes are of convenient and practical proportions for soil measurements. As a result, this method was chosen for measurements at 37 GHz.

PRINCIPLES OF A MICROWAVE BRIDGE

Fundamental Equations

The attenuation constant α and phase constant β for a TE wave in a rectangular guide can be written in the form (ref. 12)

$$\gamma = \alpha + j\beta \tag{2}$$

$$(\alpha + j\beta)^2 = \frac{2\pi}{\lambda_0}\left[\left(\frac{\lambda_0}{\lambda_c}\right)^2 - c^2\mu_0\epsilon' - j\mu_0 c^2\epsilon''\right] \tag{3}$$

$$\epsilon = \epsilon' - j\epsilon'' \tag{4}$$

where

γ = propagation constant

α = attenuation constant, Np m^{-1}

β = phase constant, rad m^{-1}

λ_0 = free space wavelength, m $= c/\nu_0$, $c = 3 \times 10^8$ m s^{-1}

$\lambda_c = a/2$ = cutoff wavelength of guide for TE_{10} mode, m, where a is width of guide, m

μ_0 = permeability of free space, 1.257×10^{-6} H m^{-1}

ϵ' = real part of dielectric constant, F m^{-1}

ϵ'' = imaginary part of dielectric constant, F m^{-1}

ϵ = permittivity of medium, F m^{-1}

Other definitions to be used are

$$\beta_0 = \frac{2\pi}{\lambda_{g0}} \tag{5}$$

$$\beta_e = \frac{2\pi}{\lambda_{ge}} \tag{6}$$

where

β_0 = propagation constant in guide for free space

β_e = propagation constant in guide with medium of permittivity ϵ

λ_{g0} = guide wavelength in free space, m

λ_{ge} = guide wavelength in medium with permittivity ϵ, m

and where

$$\lambda_{g0} = \lambda_0 \left[1 - \left(\frac{\lambda_0}{\lambda_c} \right)^2 \right]^{-1/2} \tag{7}$$

$$\lambda_{ge} = \lambda_0 \left[\frac{\epsilon}{\epsilon_0} - \left(\frac{\lambda_0}{\lambda_c} \right)^2 \right]^{-1/2} \tag{8}$$

Solving equation (3) for ϵ' and ϵ'' gives

$$\epsilon' = \frac{1}{c^2 \mu_0} \left[\left(\frac{\lambda_0}{\lambda_c} \right)^2 - \left(\frac{\lambda_0}{2\pi} \right)^2 (\alpha^2 - \beta_e^2) \right] \tag{9}$$

$$\epsilon'' = \frac{1}{c^2 \mu_0} \left(\frac{\lambda_0}{2\pi} \right)^2 2\alpha\beta \tag{10}$$

Method of Determining α and β_e

The definitions of α and β_e suggest their method of measurement. The TE wave amplitude attenuation in a sample of length L is given by $e^{-\alpha L}$. If the net power attenuation

(attenuation with sample in guide minus attenuation in the empty guide) is A dB, α can be calculated from

$$\alpha = \frac{A}{8.6L} \quad \text{Np m}^{-1} \tag{11}$$

Similarly, if the length of the sample is changed by Δl, and the accompanying phase shift in the transmitted wave is $\Delta\phi$, then

$$\beta_e = \frac{\Delta\phi}{\Delta l} + \beta_0 \tag{12}$$

Very lossy samples (losses greater than 30 dB cm^{-1} require different measurement and calculation procedures for β_e, and will therefore be discussed as a separate case. The length of the sample cell for these samples is very small, typically on the order of 0.3 to 0.5 cm. Longer sample lengths lead to very weak null signals. The short length makes it impractical as well as inaccurate to determine β_e by changing the sample length as outlined previously. As will be shown, the accurate determination of β_e depends on the condition $\Delta l \ll L$; but this condition now is no longer met because $\Delta l \sim L$. Consequently, the procedure is changed, and one determines the phase shift in the sample of length L. This shift $\Delta\phi$ is of manageable magnitude (i.e., 2π to 3π rad) and can be measured unambiguously. But this $\Delta\phi$ now determines the phase of the transmitted wave. (See detailed discussion in the section entitled "Reflection Errors.") However, if the amplitude and phase of the wave emerging from the sample are known, β_e can be calculated.

The measurement of A and $\Delta\phi$ can be done in a bridge setup in which the wave from the sample is nulled by a wave from the same source appropriately attenuated and shifted in phase.

The experimental arrangement to do this can take numerous forms. Buchanan (ref. 4) used a hybrid T as the bridge element with attenuator and phase shifter in E and H arm, respectively. The sample cell can be put in either arm. The method used here is the same in essentials but differs in the arrangement of the microwave components. (See the section entitled "Experimental Method.")

The intrinsic accuracy of the method can be estimated from equations (9) and (10), if the calibration errors of the instrument are known. Observational errors are analyzed in detail in the section entitled "Experimental Errors." The maximum errors in ϵ' and ϵ'' are

$$\delta\epsilon' = \pm\left[\frac{1}{c^2\mu_0}\left(\frac{\lambda_0}{2\pi}\right)^2\right] 2(|\alpha\, d\alpha| + |\beta_e\, d\beta_e|) \tag{13}$$

$$\delta\epsilon'' = \pm\left[\frac{1}{c^2\mu_0}\left(\frac{\lambda_0}{2\pi}\right)^2\right] 2(|\alpha\, d\beta_e| + |\beta_e\, \delta\alpha|) \tag{14}$$

where

$$\delta\beta_e = \left|\frac{\delta\Delta\phi}{\Delta l}\right| + \left|\Delta\phi\ \frac{\delta\Delta l}{\Delta l^2}\right| \tag{15}$$

$$\left.\begin{aligned}\delta\Delta\phi &= |\delta\phi_1| + |\delta\phi_2| \\ \Delta\phi &= \phi_1 - \phi_2\end{aligned}\right\} \tag{16}$$

$$\left.\begin{aligned}d\alpha &= \left|\frac{\delta A}{8.6L}\right| \\ \delta L &\sim 0\end{aligned}\right\} \tag{17}$$

The calibration accuracy (maximum values quoted by the manufacturer) of the various components is

$\delta\phi$ (phase shifter) $= \pm 1/40$ rad

$\delta\phi$ (attenuator) $= \pm 1/60$ rad

δA (phase shifter) $= \pm 0.15$ dB (measured value)

δA (attenuator) $\cong \pm 0.2$ dB

$\delta\Delta l$ $\sim 2 \times 10^{-5}$ m

The following are representative values for an "as found" soil sample:

$A = 15$ dB

$L = 12 \times 10^{-2}$ m

$\Delta\phi \sim 2$ rad

$\alpha \sim 15$ Np m^{-1}

$\beta_e \sim 10^3$ rad m^{-1}

$\Delta l = 3 \times 10^{-3}$ m

$\epsilon' \sim 2.5 \times 10^{-11}$ F m^{-1}

$\epsilon'' \sim 5.0 \times 10^{-13}$ F m^{-1}

$\nu = 37$ GHz

On the basis of these values, $\delta\alpha = \pm 0.35$ dB and $\delta\beta_e = \pm 22$ rad m^{-1}. For the maximum intrinsic errors in ϵ' and ϵ'', maximum errors are $\delta\epsilon' = \pm 6.5 \times 10^{-13}$, $\delta\epsilon'/\epsilon' = \pm 3.0$ percent, $\delta\epsilon'' = \pm 1.9 \times 10^{-14}$, and $\delta\epsilon''/\epsilon'' = \pm 3.5$ percent. Calculations on a sample of 10 percent water content indicate a maximum intrinsic accuracy of $\delta\epsilon'/\epsilon' = \pm 2.5$ percent and $\delta\epsilon''/\epsilon'' = \pm 2.0$ percent.

Very lossy samples (water content greater than 10 percent and attenuation greater than 30 dB cm^{-1}) tend to show considerably larger errors. The primary reason for that is the rather short sample length L used in the measurements. Thus a 13.5-percent sample gives $\delta\epsilon'/\epsilon' = \pm 3.5$ percent max and $\delta\epsilon''/\epsilon'' = \pm 4.0$ percent max. The same type of sample with 20 percent water content shows a maximum error of ±6.0 percent for ϵ' and ±7.0 percent for ϵ''. A summary of these results and pertinent data are given in table 2, which appears later in this document.

Equations (9) and (10) for the determination of ϵ' and ϵ'' are correct if the correct values of α and β_e have been determined. But equation (11) for the determination of α in fact determines the amplitude of the wave transmitted by the sample, and neglects reflections at the sample interfaces. Further, equation (12) for the determination of the propagation constant β_e in effect determines the phase shift of two transmitted waves corresponding to two different lengths of sample. It also is an approximation, but a very close one. Therefore one must investigate the effect of reflections on the calculation of α and ascertain the conditions for proper determination of β_e.

The problem of finding the transmitted wave for an electromagnetic wave incident on a dielectric plate has been solved many times and in many different ways (refs. 13 to 15). The following discussion briefly sketches the solution of the problem and gives the result, using a notation and definitions suitable for the problem. The method is similar to the derivation of the Fabry-Perot interferometer equations (ref. 13), with concepts borrowed from the solution of Maxwell's equations. The angle of incidence of the wave is 0° (normal incidence), the transverse components of the wave are in the x-y plane, and the direction of propagation is in the $+z$ direction. Let the incident electric wave be $E_{0x}e^{-\gamma z}$, $\gamma = \alpha + j\beta$, and assume that at $z = 0$, $E_{0x}e^{-\gamma z} = 1$. Let R be the complex amplitude reflection coefficient of the wave in medium 1 incident on medium 2. R' is the complex amplitude reflection coefficient of a wave in medium 2 incident on medium 1. (See fig. 1.) The amplitudes of the various transmitted and reflected waves can be evaluated at each point from the boundary conditions--the continuity of the tangential component of the electric field. For the total transmitted amplitude at $z = +L$

$$E^{(t)} = (1 + R)(1 + R')e^{-\gamma L}(1 + R'^2e^{-2\gamma L} + R'^4e^{-4\gamma L} + \cdots) \tag{18}$$

Summing the geometric series for an infinite number of terms results in

$$E^{(t)} = \frac{(1 - R^2)e^{-\gamma L}}{1 - R'^2e^{-2\gamma L}} \tag{19}$$

If medium 3 is the same as medium 2, $R = -R'$ and

$$E^{(t)} = \frac{(1 - R^2)e^{-\gamma L}}{1 - R^2e^{-2\gamma L}} \tag{20}$$

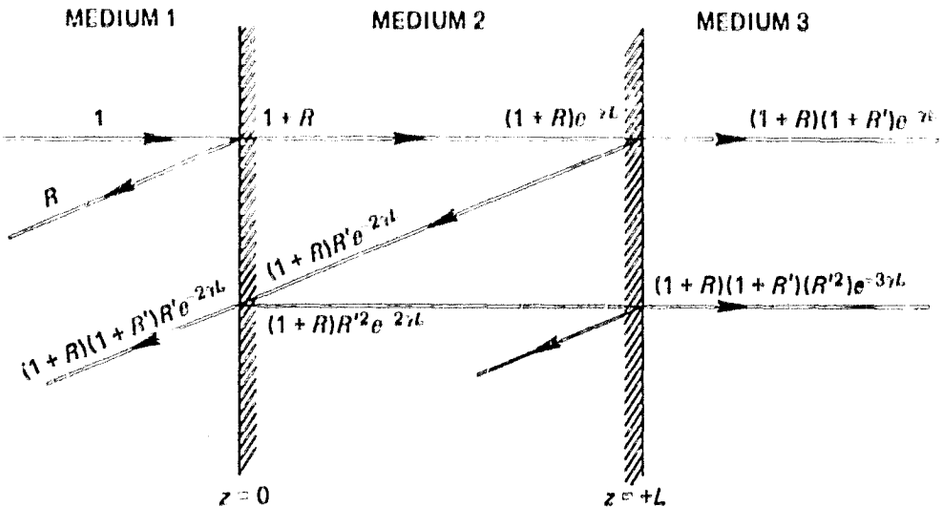

Figure 1.—Amplitudes of waves transmitted and reflected at sample interfaces.

For the condition $|e^{-2\gamma L}| \ll l$, which can be arranged by making the sample cell length L long enough, one can neglect the interference term $(1 - R^2 e^{-2\gamma L})$, and therefore

$$E^{(t)} = (1 - R^2)e^{-\gamma L}$$

$$= (1 - R^2)e^{-(\alpha + j\beta)L} \tag{21}$$

The solution of this equation for α and the limitation that equation (20) places on the determination of β_e by equation (12) are discussed in the section entitled "Reflection Errors."

EXPERIMENTAL METHOD

Description of the Microwave Bridge

Figure 2 shows a schematic diagram of the 37-GHz twin-arm microwave bridge suggested by T. Wilheit (personal communication). Attenuator and phase shifter are of the rotary vane type.[2] The microwave cw signal was 100-percent square-wave modulated at 1000 Hz and detected by a 1N53 crystal and a tuned SWR meter. The microwave source is a backward wave oscillator with a maximum output of approximately 20 to 25 mW. The unattenuated power reaching the crystal through the reference arm is about 11.5 dB down from 25 mW, considering losses in isolators, components, and a 3-dB power division in the hybrid T's.

The detected noise level output is approximately 0.06 μW at a 1-μW signal level, so that the maximum sample attenuation should not exceed 40 dB for a reasonably accurate null reading. The noise level is independent of the modulation frequency, indicating that the observed noise is probably mostly FM noise rather than $1/f$ crystal noise. Use of a lock-in amplifier did not substantially improve the detection sensitivity.

[2]Specific equipment was a signal generator 650/659, Alfred Electronics, Inc.; cavity DBD-720-1, Demornay Microwave Products, Systron-Donner Corp.; precision phase shifter TRG K-528, TRG Division, Control Data Corp.; and a precision attenuator HP R382A and SWR meter HP 415B, Hewlett-Packard Co.

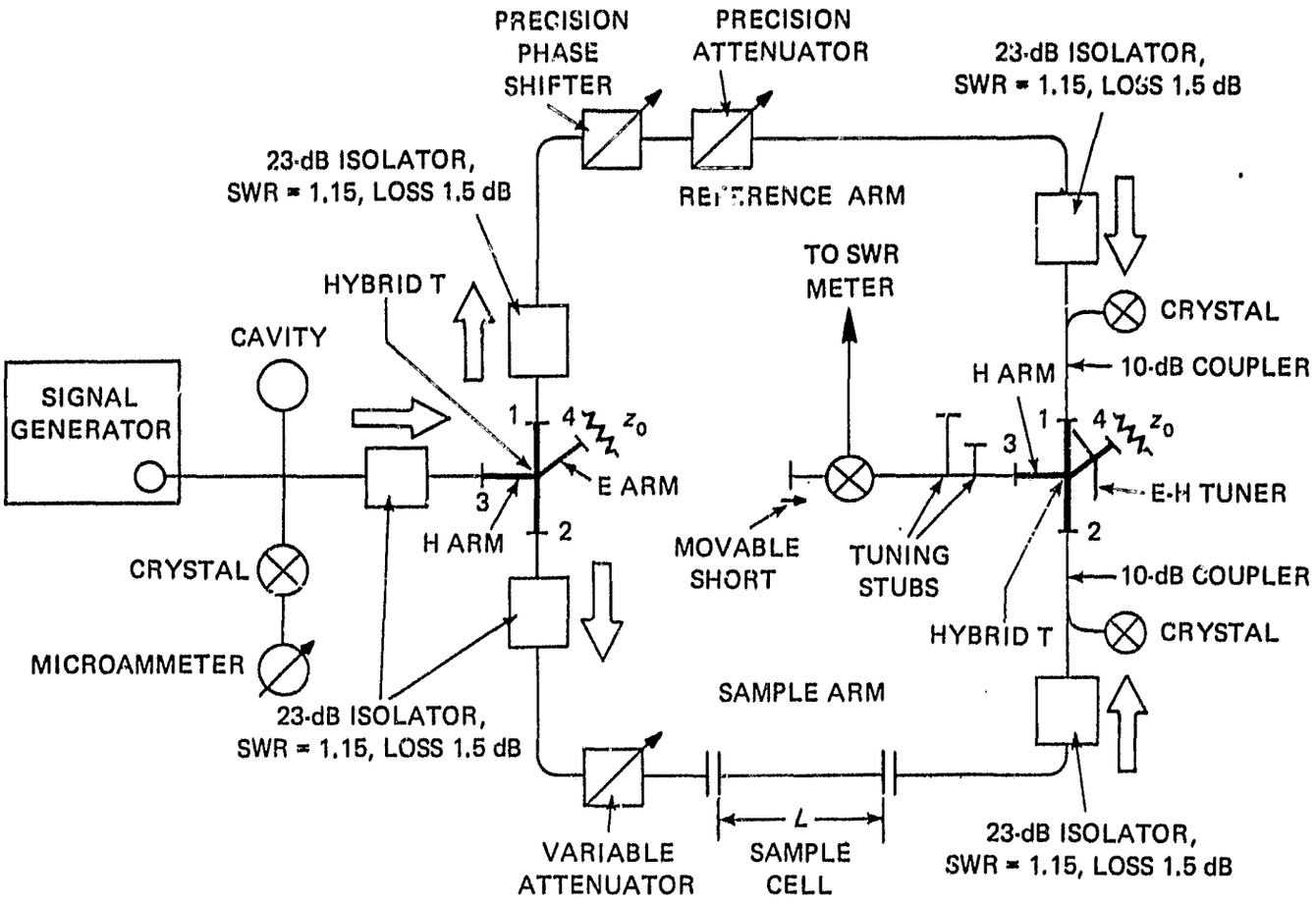

Figure 2.--Schematic diagram of twin-arm microwave bridge. Specific equipment is identified in the text.

There are two hybrid T's in the bridge, the first used as a power divider, the second as a signal comparator. Because proper use of the T's is of great importance in the operation of the bridge, a detailed analysis of their operation is given.

The properties of the hybrid T are best examined by means of its scattering matrix **S** (ref. 16). The scattering matrix of a T is

$$\mathbf{S} = (S_{ij}) \qquad i,j = 1, 2, 3, 4 \ldots \tag{22}$$

where S_{ij} are the scattering coefficients and where subscripts 1 and 2 refer to the two collinear H arms, 3 to the H arm (coplanar with arms 1 and 2), and 4 to the E arm. For match-terminated ports, the coefficients have the following properties: $S_{ij} = S_{ji}$, $S_{13} = S_{23}$, $S_{14} = -S_{24}$, $S_{11} = S_{22}$, and $S_{34} = 0$. From $S_{13} = S_{23}$ it follows then that power into port 3 divides equally between arms 1 and 2. However, if the reflection coefficients of the loads terminating ports 1 and 2 change, the power division will also change. By putting isolators in arms 1 and 2 (see fig. 2) the T essentially sees a match-terminated port, and power division remains unaffected by the changing of reflection coefficients in the sample arm

(due to different samples) and the rather small variations in the reference arm.[3] The important criterion is not equal power division but constancy of power division. The power division is a constant at a given frequency but may change with frequency. The second hybrid T compares the signals from the reference and sample arm, and the analysis of its performance is somewhat trickier. There are obviously two conditions that are desirable for this T: (1) maximum signal power from both arms 1 and 2 into arm 3, and (2) constant power division. It can easily be shown (ref. 16) for a hybrid T that the voltage at the detector is

$$E_{03} = S_{i3}(E_{i1} - E_{i2}) \tag{23}$$

where E_{i1} and E_{i2} are the input voltages to arms 1 and 2, respectively. This equation is true whether or not the T is matched (i.e., a magic T). If the T is not matched (i.e., a hybrid T), then as in the case of the first T, interaction between the T and the load (primarily the soil sample) will take place. This interaction will affect the voltage at the detector and cause a false reading of magnitude and phase of the wave transmitted by the sample. The solution, as in the case of the first T, is to use isolators in arms 1 and 2. One can calculate the power into arm 3 from (ref. 16)

$$|S_{11}|^2 + |S_{12}|^2 + |S_{13}|^2 + |S_{14}|^2 = 1 \tag{24}$$

Then

$$|S_{13}|^2 = |S_{23}|^2$$

$$= 1 - (|S_{14}|^2 + |S_{12}|^2 + |S_{11}|^2 \tag{25}$$

i.e., the power into arm 3, which is proportional to $|S_{13}|^2$ may, depending on the magnitude of S_{14}, S_{12}, and S_{11} be considerably less than 1. In a perfectly matched T, $S_{12} = S_{11} = 0$ and $|S_{14}|^2 = 1/2$.

Hence the optimum signal power into arm 3 is 1/2 of the incident power, and consequently for an unmatched T will be much less.[3] But T's are never perfectly matched—those commercially available have a VSWR in arms 1 and 2 of approximately 1.4 to 1.7; and furthermore, the VSWR is fairly frequency dependent. In other words, even in a matched T, some interaction between the T and the loads in arms 1 and 2 will take place. A detailed theoretical investigation has been made of the effect of load VSWR (or reflection coefficient), matched and unmatched T's, and introduction of isolators, coupled with an experimental determination of $|S_{12}|$, $|S_{13}|$, $|S_{14}|$, and $|S_{11}|$. Results of this study will be published elsewhere.[3] Suffice it to say, the problem was solved by using an unmatched T (see fig. 2), and introducing conventional matching devices in arms 3 and 4 to optimize power into arm 3, or to make $|S_{11}| \cong |S_{22}| \cong |S_{12}| \cong |S_{21}| \cong 0$.

Clearly, the matching devices must not destroy the symmetry of the T. (Otherwise the T becomes just an asymmetrical four-port device, and the properties of **S** of equation (22) become completely irrelevant.) It is easy enough to make an adjustable double stub tuner or

[3]Report in preparation.

use a commercial stub tuner in H arm 3 to meet the symmetry requirements. The E arm tuning element, in order to preserve the symmetry of the T, would have to be introduced into the narrow wall of the E arm; i.e., an adjustable inductive post or adjustable H-plane stub. It was found, however, that an E-H tuner in the E arm, although asymmetric with respect to the symmetry plane of the T, is adequate as a matching element.

Values in the list following were obtained for the 37-GHz bridge, which shows that adequate isolation between 1 and 2 and 2 and 1 was achieved, as well as small and almost equal reflections from the collinear arms; i.e., $|S_{11}|^2 = |S_{22}|^2$. (All figures are relative to $|S_{13}|^2$.)

Detector arm 3	$\|S_{13}\|^2$	0.01
	$\|S_{23}\|^2$	0.016
Reference arm 1	$\|S_{11}\|^2$	0.002
Sample arm 2	$\|S_{22}\|^2$	0.0025
Collinear arms	$\|S_{12}\|^2$	0.00016
	$\|S_{21}\|^2$	0.0001

Although no measurements were made of the power into arms 1 and 2, a conservative estimate can be made of the VSWR corresponding to the relative values of $|S_{13}|^2$ and $|S_{11}|^2$. The value of the VSWR from arms 1 and 2 is found to be approximately 1.6, comparable to commercially available magic T's.

The possibility of using hybrid T's as signal comparators in broadband applications and their limitations will be discussed elsewhere.[4]

Sample Cell

Sample cells were constructed of standard waveguide components; choke-to-choke adaptors were used to clamp mica windows to the cover flanges of the test cell waveguide; cover-to-cover adaptors provided precision components for changing the length of the cell for the measurement of $\beta_e = \Delta\phi/\Delta l$. Sample cell lengths were held within ±0.0025 cm (±0.001 in.). To cover the range of α as a function of moisture content, five sample cells were made of lengths 11.295, 3.1700, 2.0320, 1.021, and 0.511 cm. Figure 3 shows a dia-

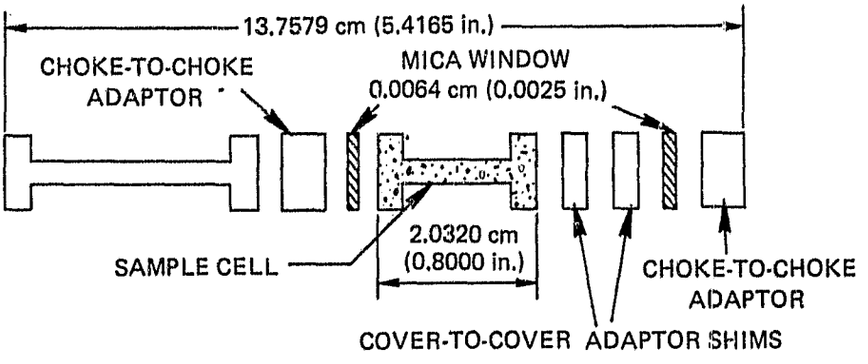

Figure 3.—Microwave specimen cell for 37-GHz measurements.

[4]Report in preparation.

gram of a typical cell. The overall length of the cell was always the same; i.e., 13.7579 cm (5.4165 in.) for 37 GHz, held to close tolerances of ±0.0025 cm (±0.001 in.). This allowed for easy interchange of all cells in the bridge.

Sample Preparation and Experimental Procedure

"As found" soil samples held some moisture, depending on ambient humidity. Samples were therefore dried. Oven drying, even prolonged heating (20 hr at 393 K (120° C)) removed only 2/3 of the moisture (by weight). Vacuum drying was therefore used on all samples before any measurements were made or any distilled water was added. Samples were vacuum dried for several hours with a small mechanical pump in series with a flask containing 500 g of Dryrite.[5] The method of filling the waveguide sample cell was empirical--it consisted primarily of vigorous tapping and shaking of the cell as the sample was gradually added. Measurement points recorded on the graphs (figs. 6 to 8, shown later) represent independent determinations; i.e., the soil sample was removed from the cell and replaced by a fresh sample from the same prepared batch. Relatively large pieces of rock, wood, or clumps of soil were eliminated or broken up. All moisture percentages were by weight based on the dry weight of the soil. Moisture measurements were made to within 0.2 to 0.5 percent. Maintaining the moisture content while filling the guide is an obvious problem. Extreme care was used to expose the moist soil to the air as little as possible. The sample guide was sealed off with plastic tape between fillings and during tapping and shaking of the cell.

Phase angle changes produced by removing the sample from the 3- or 6-mm shims of the cell (see fig. 3) were less than 360° to avoid ambiguities in the phase angle readings. At high moisture contents the usual procedure was to determine accurately the phase shift for 3 or 6 mm of sample, and then check this figure against a 1-mm change. A phase change of 360° in 1 mm requires a dielectric constant ϵ' of 64 at 37 GHz—greater than that of pure water.

To make a direct assessment of the bridge's accuracy aside from the intrinsic accuracy calculations, the specimen cell was replaced by a combination precision attenuator and sliding short. This combination permitted simulation of absorption and phase shift. The sample arm precision attenuator was changed over a range from 0 to 20 dB at 1-dB intervals. Its readings checked the reference arm attenuator to within ±0.1 dB, except two points of deviation to ±0.2 dB. The phase errors determined by the micrometer sliding short were ±4°. However, the standing wave produced by the 30-dB reflectivity of a 10-dB coupler used in this measurement accounts for ±2°. This is in fair agreement with the calibration accuracy of ±1.5° of the reference arm rotary phase shifter.

REFLECTION ERRORS

An expression for the electromagnetic wave transmission of the sample in the guide was derived in the previous section. The measurement of β_e consists in finding the phase shift

[5]A registered trademark of the W. A. Hammond Dryrite Co.

between two transmitted waves. Let the first wave traverse a length L_1 and the second L_2; then from equation (20)

$$E_1^{(t)} = \frac{(1 - R^2)e^{-\gamma L_1}}{1 - R^2 e^{-2\gamma L_1}} \tag{20a}$$

$$E_2^{(t)} = \frac{(1 - R^2)e^{-\gamma L_2}}{1 - R^2 e^{-2\gamma L_2}} \tag{20b}$$

These equations show very clearly that the phase change $\Delta\phi$ between $E_1^{(t)}$ and $E_2^{(t)}$ is given by

$$\Delta\phi = (L_1 - L_2)(\beta_e - \beta_0) \tag{26}$$

only if $1 - R^2 e^{-2\gamma L}$ remains constant, which is true if

$$\Delta l \ll L \tag{27a}$$

Variations in $1 - R^2 e^{-2\gamma L}$ are also minimized by the condition

$$|e^{-2\gamma L}| \ll 1 \tag{27b}$$

which must be met to allow calculation of α from equation (21). When $\Delta l \sim L$, as in the case of high-loss samples, equation (26) is not quite applicable, and β_e is calculated by an iteration procedure together with α from equation (21).

It remains to find the effect of the "correction factor" $1 - R^2$ of equation (21) on the value of α. Before proceeding to a direct solution of equation (21), it will be instructive and useful to solve the problem for a given reflection coefficient and calculate the $\Delta\alpha$ due to reflections. It will also be useful to calculate the difference between $\beta_e L$ and the phase $\Phi = \eta L$ of the transmitted wave. From equation (21)

$$(1 - R^2)e^{-(\alpha + j\beta)L} = Ae^{-j\Phi} \tag{28}$$

where A is as defined in equation (11). Set $A = e^{-\alpha' L}$, and let $\Delta\alpha = \alpha' - \alpha$ and $\Delta\beta = \eta - \beta$, where $\Delta\alpha$ and $\Delta\beta$ are not necessarily small quantities, and the result is

$$1 - R^2 = e^{-(\Delta\alpha + j\Delta\beta)L} \tag{29}$$

Writing $R^2 = |R|^2 e^{2j\theta}$ and solving equation (29) for $\Delta\beta L$ and $\Delta\alpha L$ results in

$$\cot \Delta\beta L = \frac{1 - |R|^2 \cos 2\theta}{|R|^2 \sin 2\theta} \tag{30}$$

$$\Delta\alpha L = -\frac{1}{2} \ln (1 - 2|R|^2 \cos 2\theta) \tag{31}$$

Let $1 - |R|^2 e^{2j\theta} = ce^{j\chi}$; then consideration shows that for $\pi/2 \leq \theta \leq \pi$ and $0 \leq \theta \leq \pi/2$, χ varies from $0 \leq \chi \leq \pi/2$ to $-\pi/2 \leq \chi \leq 0$, respectively. Because $\chi = -\Delta\beta L$, then $|\Delta\beta L| \leq \pi/2$

and $|\Delta\beta L|$ is bounded. Figures 4 and 5 show plots of $\Delta\beta L$ and $\Delta\alpha L$, respectively, as functions of both $|R|^2$ and θ. They show that even for a relatively large reflection coefficient ($|R|^2 \sim 0.3$, or 10 dB), $|\Delta\beta L| \sim 0.3$; for representative values of β and L, $\Delta\beta/\beta \ll 1$, or $\eta \sim \beta$. This property is useful in the solution of equation (28). The case for $\Delta\alpha L$ is different $\Delta\alpha L$ increases without limit, as it obviously must as $|R|^2$ approaches 1. From the curves, it is seen that $\Delta\alpha$ is comparable or larger than the $\delta\alpha$ due to intrinsic errors. Reflection corrections are therefore required.

The solution of equation (28) presents some difficulties. As will be seen in equations (32) and (33), and has been seen in equations (9) and (10), R can be expressed explicitly as $R(\alpha, \beta)$. Equation (28) is then a complex transcendental equation of degree six in α and β. A closed solution of this equation is impossible and it must be solved by iteration. However, an approximate calculation of R from α' and β_e and substitution in equation (28) with $\Phi \sim \beta_e L$ will give a very close approximation to α.

The solution of equation (28) by iteration then should present no difficulties. An analytic proof of the convergence of the iteration is presented in appendix A. However, it has been assumed so far that all quantities except α are known in equation (28). But Φ is not. It is difficult to measure without ambiguity because it involves an angle on the order of a thousand degrees, but our preceding analysis shows that $\Phi \sim \beta_e L$, and is not very sensitive to changes in R. (See fig. 5.) It will therefore be possible to obtain an iterated solution of α while calculating the correct value of Φ by the same iteration.

The iteration proceeds as follows: Calculate ϵ' and ϵ'' using equations (9) and (10) and the approximate values of α and α'. A first approximation to R and $R^{(1)}$ is obtained from the equation

$$R^{(1)} = \frac{Z^{(1)}(\alpha', \beta_e) - Z_0}{Z^{(1)}(\alpha', \beta_e) + Z_0} \tag{32}$$

where $Z^{(1)}(\alpha, \beta_e)$ is the wave impedance for the TE mode

$$Z^{(1)}(\alpha, \beta_e) = \frac{(2\pi/\lambda_0)(\mu_c/\epsilon_c)^{1/2}\beta_e[1 + j(\alpha/\beta_e)]}{\alpha^2 + \beta_e^2} \tag{33}$$

and Z_0 is the characteristic impedance of the guide

$$Z_0 = \frac{\lambda_{g0}}{\lambda_0}\sqrt{\frac{\mu_0}{\epsilon_0}} \tag{34}$$

All symbols are as defined previously. (The subject of waveguide reflection coefficients is treated very obscurely in the literature; only Schelkunoff (ref. 17) gives a fairly clear discussion, although Goubau (ref. 15) is clear once one gets past the notation.) In the calculation of R, the wave impedance of the sample was used rather than its input load impedance Z_L, a justifiable procedure because there is always enough attenuation in the sample so that $Z(\alpha, \beta)$ approximates Z_L very closely. The first approximation to R is now substituted in

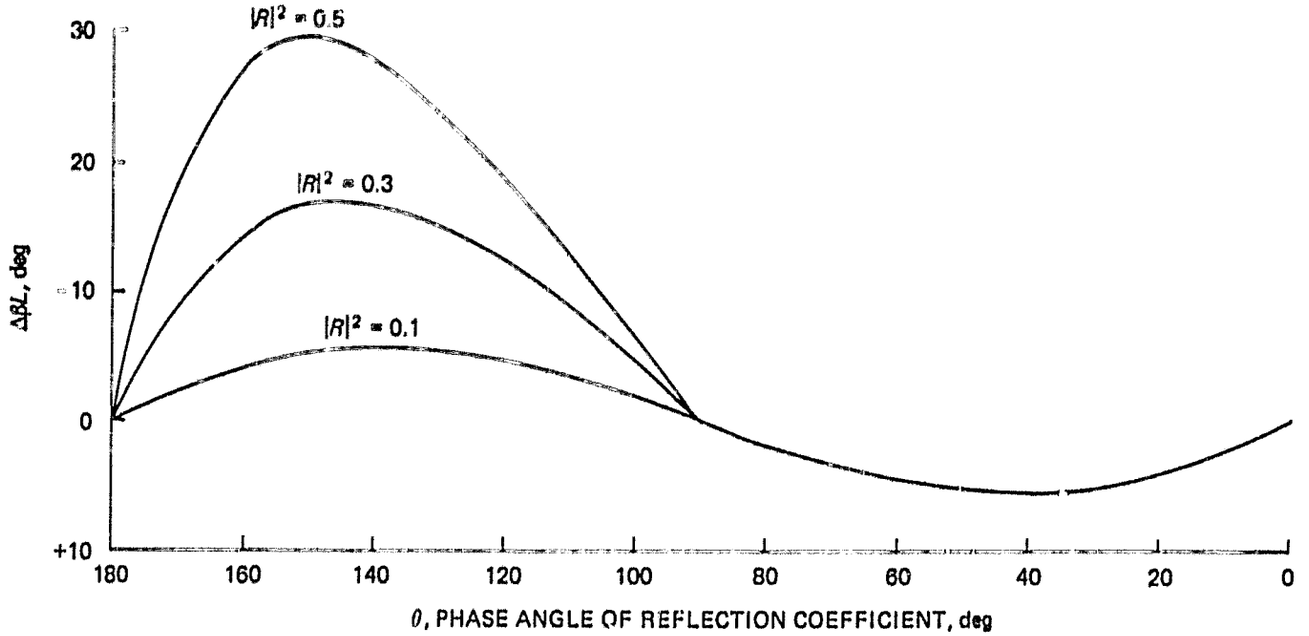

Figure 4.—Phase angle change versus phase angle of reflection coefficient.

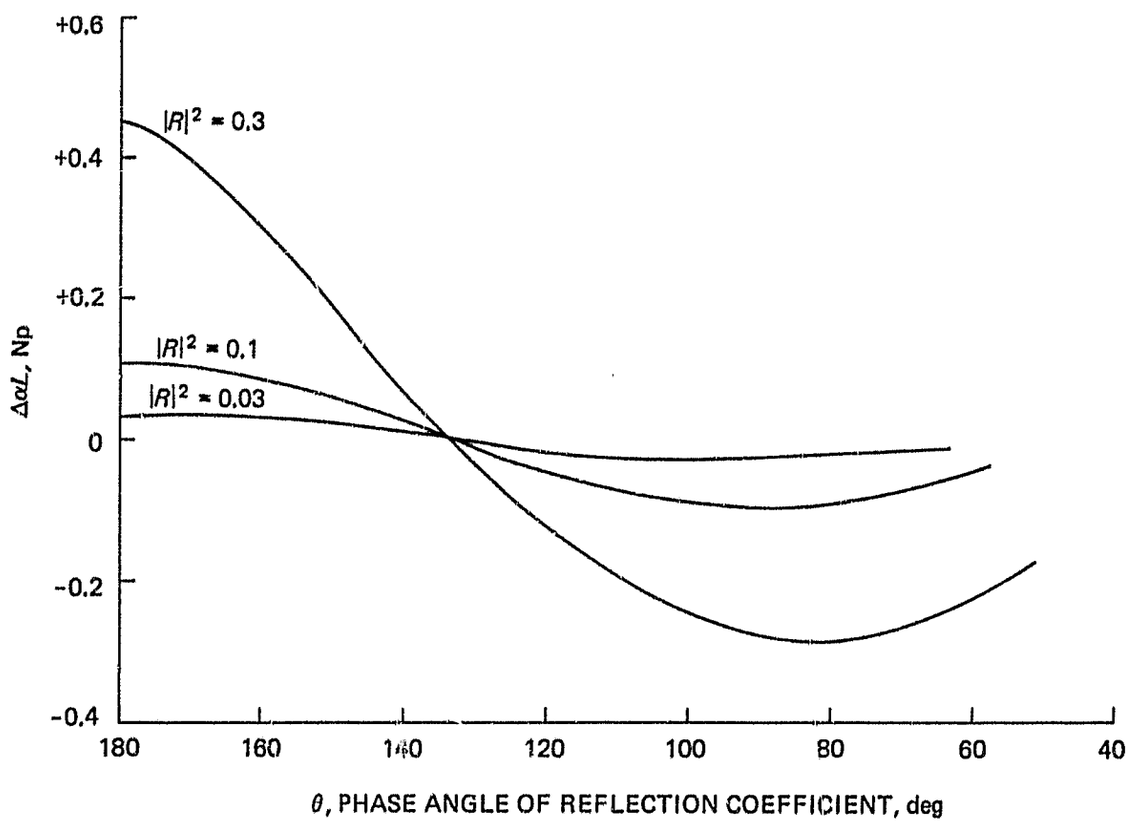

Figure 5.—Attenuation constant versus phase angle of reflection coefficient.

equation (28) for α and Φ to obtain a second approximation to α, $\alpha^{(2)}$ and a first approximation to Φ, $\Phi^{(1)}$. The general iteration equation is clearly

$$(1 - |R|^{(i)2} e^{2j\theta^{(i)}}) e^{-\alpha^{(i+1)}L} e^{j\Phi^{(i)}} = e^{-\alpha' L} e^{j\beta_e L} \tag{35}$$

The expression on the right remains constant throughout the iteration.

For relatively low-loss samples (moisture content less than about 10 percent), direct determination of β_e was possible. The conditions for this determination were given in equations (27a) and (27b). High-loss samples require a different procedure, because it is no longer possible to satisfy equation (27a). In fact, it becomes more convenient and straightforward simply to determine the phase shift of the transmitted wave in length L of the sample and then determine β_e from equation (28). Two measurements are made as before, the first measurement with the sample in the cell of length L. The equation for the transmitted wave is then, from equation (28),

$$(1 - R^2) e^{-(\alpha + j\beta_e)L} = e^{-\alpha' L} e^{-j\eta L} \tag{36}$$

A second measurement without the sample gives $e^{-j\beta_0 L}$ for the transmitted beam. If the phase determination for the first measurement gives Φ_1, Φ_2 for the second, and $\Delta\Phi = \Phi_1 - \Phi_2$, then clearly, from equation (36)

$$\Delta\Phi = \eta L - \beta_0 L$$

$$\eta = \frac{\Delta\phi}{L} + \frac{2\pi}{\lambda_{g0}}$$

In other words, in equation (36) the quantities α' and η are now known and it remains to find α and β_e. From the preceding analysis, it was found that $\eta \sim \beta_e$. In fact, from figure 4 one can estimate for $R \sim -0.5\ \angle 170°$ that $\Delta\beta = 50$ rad m^{-1} if $L = 3 \times 10^{-3}$ m. One can therefore formulate the iteration equation for α and β_e by writing equation (35) in the form

$$(1 - R^{(i)2}) e^{-\alpha^{(i+1)}L} e^{-j\beta_e{}^{(i+1)}L} = e^{-\alpha' L} e^{-j\eta L}$$

and setting $\beta^{(1)} = \eta$ and $\alpha^{(1)} = \alpha'$.

The condition for convergence of the iteration equation is given by

$$\left| \frac{2R}{L} \frac{\partial R}{\partial \alpha} \right| < 1 \tag{37}$$

Equation (37) is derived in appendix A. For a very lossy sample (15 percent water content)

$$\frac{\partial R}{\partial \alpha} \sim 10^{-5}$$

and

$$L > \left| 2R \frac{\partial R}{\partial \alpha} \right| = 1 \times 10^{-5} \text{ m}$$

Hence convergence is assured for even very short sample lengths.

Table 1 is a reproduction of a computer printout of successive iterations for samples with various water contents. As expected, the first iteration results in values of α, ϵ', and ϵ'' (and β_e for very lossy samples) that differ little from subsequent iterations. R' and R'' are the real and imaginary parts of the reflection coefficient $R = R' + jR''$.

Reflection corrections for relatively low-loss samples (less than 10 percent water) are generally small compared to intrinsic and observational errors. The real part of ϵ is almost unaffected by α, β being very much larger than α. Hence corrections to ϵ' are too small to be of importance in this low water content range. For the imaginary part of ϵ, which is directly proportional to α, the correction can amount to several percent.

Very lossy samples (moisture content over 10 percent) require correction in α as well as β_e as shown previously. The constants α and β_e are now of the same order of magnitude, and, consequently, there will be substantial corrections of both ϵ' and ϵ''. As expected, the measured α (i.e., α') is much too high, and the measured dielectric constant ϵ', too low. Oddly enough, the correction of ϵ'' is less than expected because the decrease in α is partially compensated by an increase in β_e. Reflection corrections for α and β_e are approximately 10 and 1 percent, respectively.

EXPERIMENTAL ERRORS

The intrinsic accuracy of the method, discussed previously, is the maximum accuracy obtainable considering calibration errors of attenuators, phase shifters, and measurement errors in the cell lengths (and shim lengths). In this section, the error calculations are concluded by considering in addition the observational errors. (Errors in the determination of λ_0 and λ_{g0} are not considered because they are very small compared to all other errors.) This classification of errors is somewhat arbitrary but useful. Observational errors in the reading of A and ϕ change with the changing ratio of detected signal level to detected noise in the crystal null detector. Intrinsic and observational errors are considered statistically independent and are combined by calculating the rms error in ϵ from

$$\delta\epsilon_{\text{rms}} = \sqrt{\left(\frac{\partial\epsilon}{\partial\alpha}\,\delta\alpha\right)^2 + \left(\frac{\partial\epsilon}{\partial\beta}\,\delta\beta\right)^2} \tag{38}$$

where $\delta^2\alpha = \delta^2\alpha_1 + \delta^2\alpha_2$ and where $\delta\alpha_1$ is the estimated intrinsic and $\delta\alpha_2$ the estimated mean observational error. The process is similar for β.

The calculation of $\delta\epsilon_{\text{rms}}$ is rather tedious and its details are omitted. Calculations were made for samples with representative moisture contents (i.e., 0.6, 10, 13.5, and 20 percent). Errors for other moisture concentrations were assumed to be between the appropriate limits. Table 2 summarizes the results and shows both maximum intrinsic errors and total rms errors. Graphs of ϵ versus percent of water show scatter that in many cases far exceeds the rms error. This experimental point scatter is clearly caused by difficulties of getting reproducible samples and reproducible sample packing.

Table 1.—Computer Iteration of α, η, $\epsilon = \epsilon' - j\epsilon''$, $R = R' + jR''$, and β_ϵ for Loamy Fine Sand, Sample M5

$\alpha^{(i)}$	$\eta^{(i)}$	$\epsilon^{(i)\prime}$	$\epsilon^{(i)\prime\prime}$	$R^{(i)\prime}$	$R^{(i)\prime\prime}$	$\beta_\epsilon^{(i)}$
			Vacuum dried			
0.853035E 01	0.125342E 04	0.259896E-10	0.314563E-12	-0.327365E 00	0.303809E-02	0.125344E 04
0.755384E 01	0.125342E 04	0.259891E-10	0.278549E-12	-0.327355E 00	0.269037E-02	0.125344E 04
0.755387E 01	0.125342E 04	0.259892E-10	0.278551E-12	-0.327356E 00	0.269037E-02	0.125344E 04
0.755387E 01	0.125342E 04	0.259892E-10	0.278551E-12	-0.327356E 00	0.269037E-02	0.125344E 04
0.755387E 01	0.125342E 04	0.259892E-10	0.278551E-12	-0.327356E 00	0.269037E-02	0.125344E 04
			5 percent H_2O			
0.987670E 02	0.114629E 04	0.221006E-10	0.333386E-11	-0.289499E 00	0.393675E-01	0.114735E 04
0.951164E 02	0.114633E 04	0.220753E-10	0.320763E-11	-0.288921E 00	0.379658E-01	0.114735E 04
0.951260E 02	0.114633E 04	0.220766E-10	0.320809E-11	-0.288937E 00	0.379679E-01	0.114735E 04
0.951255E 02	0.114633E 04	0.220765E-10	0.320807E-11	-0.288937E 00	0.379678E-01	0.114735E 04
0.951255E 02	0.114633E 04	0.220766E-10	0.320807E-11	-0.288937E 00	0.379678E-01	0.114735E 04
$\alpha^{(i)}$	$\beta_\epsilon^{(i)}$	$\epsilon^{(i)\prime}$	$\epsilon^{(i)\prime\prime}$	$R^{(i)\prime}$	$R^{(i)\prime\prime}$	$\eta^{(i)}$
			20 percent H_2O			
0.725476E 03	0.226968E 04	0.709152E-10	0.484426E-10	-0.588347E 00	0.102808E 00	0.226968E 04
0.646658E 03	0.230493E 04	0.748396E-10	0.439858E-10	-0.587970E 00	0.909035E-01	0.226968E 04
0.647433E 03	0.230099E 04	0.745960E-10	0.438276E-10	-0.587396E 00	0.909801E-01	0.226968E 04
0.647630E 03	0.230095E 04	0.745898E-10	0.438403E-10	-0.587403E 00	0.910074E-01	0.226968E 04
0.647630E 03	0.230096E 04	0.745904E-10	0.438405E-10	-0.587404E 00	0.910068E-01	0.226968E 04
0.647630E 03	0.230096E 04	0.745904E-10	0.438404E-10	-0.587404E 00	0.910068E-01	0.226968E 04
0.647630E 03	0.230096E 04	0.745904E-10	0.438404E-10	-0.587404E 00	0.910068E-01	0.226968E 04
			30 percent H_2O			
0.903466E 03	0.236873E 04	0.734085E-10	0.629602E-10	-0.612174E 00	0.116643E 00	0.236873E 04
0.820549E 03	0.241177E 04	0.785378E-10	0.582209E-10	-0.611258E 00	0.104688E 00	0.236873E 04
0.819177E 03	0.240751E 04	0.782691E-10	0.580211E-10	-0.610701E 00	0.104810E 00	0.236873E 04
0.819388E 03	0.240748E 04	0.782617E-10	0.580352E-10	-0.610710E 00	0.104835E 00	0.236873E 04
0.819388E 03	0.240749E 04	0.782624E-10	0.580354E-10	-0.610711E 00	0.104835E 00	0.236873E 04
0.819387E 03	0.240749E 04	0.782624E-10	0.580354E-10	-0.610711E 00	0.104835E 00	0.236873E 04
0.819387E 03	0.240749E 04	0.782624E-10	0.580354E-10	-0.610711E 00	0.104835E 00	0.236873E 04

Table 2.- Representative Errors and Correction Factors

Sample	Maximum intrinsic error,[a] percent		Total rms error, percent		Reflection correction,[b] percent	
	$\delta\epsilon'$	$\delta\epsilon''$	$\delta\epsilon'_{rms}$	$\delta\epsilon''_{rms}$	$\delta\epsilon'$	$\delta\epsilon''$
M5, as found, 0.66 percent H_2O, $\alpha = 15$ Np m^{-1}, $\beta \sim 10^3$ rad m^{-1}, $L \sim 12 \times 10^{-2}$ m, $\Delta\phi \sim 2$ rad, $\Delta l \sim 3 \times 10^{-3}$ m, $\epsilon' = 2.4 \times 10^{-11}$, $\epsilon'' = 5.5 \times 10^{-13}$	±3.0	+2.5	±3.6	±3.5	0.0	-6
M5, 10 percent H_2O, $\alpha \sim 300$ Np m^{-1}, $\beta \sim 1500$ rad m^{-1}, $L \sim 1.5 \times 10^{-2}$ m, $\Delta l \sim 3 \times 10^{-3}$ m, $\Delta\phi \sim 3$ rad, $\epsilon' = 4.0 \times 10^{-11}$, $\epsilon'' = 1.5 \times 10^{-11}$	±2.0	±2.0	±3.5	±2.5	-0.3	-6
F2, 13.5 percent H_2O, $\alpha \sim 440$ Np m^{-1}, $\beta \sim 1900$ rad m^{-1}, $L \sim 5 \times 10^{-3}$ m, $\Delta\phi \sim 6.5$ rad, $\epsilon' = 5.5 \times 10^{-11}$, $\epsilon'' = 2.5 \times 10^{-11}$	±3.3	±4.0	±3.3	±3.0	+3.5	-12
F2, 20 percent H_2O, $\alpha \sim 700$ Np m^{-1}, $\beta \sim 2300$ rad m^{-1}, $L \sim 3 \times 10^{-3}$ m, $\Delta\phi \sim 5.3$ rad, $\epsilon' = 7.3 \times 10^{-11}$, $\epsilon'' = 4.3 \times 10^{-11}$	±6.0	±7.0	±5.6	±6.0	+5	-10

[a]See section entitled "Method of Determining α and β_e."
[b]See section entitled "Reflection Errors."

DISCUSSION OF RESULTS

Published data on dielectric constants of soils with varying water contents are somewhat meager. The first published results of soils with a number of different moisture percentages in the rf range (at 10 MHz) seem to have been those of Smith-Rose (ref. 18). Some of the first microwave measurements apparently were made by Ford and Oliver (ref. 19) at 9 cm on dry and "very wet" soil. They used a combination of in situ reflection and absorption between receiver and generator antennas. More recent are the X-band measurements on dry soils, and soils with 6, 10, and 25 percent water by Straiton and Tolbert (ref. 5) and by von Hippel (ref. 20) on 2, 4, and 16 percent water-content samples. There is a solitary measurement at 19 GHz on dry sand by Hertel, Straiton, and Tolbert (ref. 10).

Interestingly enough, dry soil samples taken from diverse and obscure locations and of various compositions show a surprising degree of agreement in the value of ϵ. Measurements by Straiton and Tolbert (ref. 5) show a variation from 2.5 to 2.85 $\times 10^{-11}$ F m^{-1}, von Hippel's (ref. 20) from 1.9 to 2.2 $\times 10^{-11}$, and this study at 37 GHz for three soil samples gave values from 2.5 to 2.7 $\times 10^{-11}$. However, the recent results by Wiebe (ref. 21) at

X-band on soil samples from Texas show dry soil values substantially higher than the above, some as high as 3.9×10^{-11}.

With added water, there is a radical departure of values found in this study from those in published data. Dielectric constants ϵ' ranged from 3.2 to 4.5×10^{-11} F m^{-1} at 10 percent water; the corresponding values of Wiebe show a spread from 4.5 to 8×10^{-11}. At a moisture content of 30 percent, the disparity becomes even greater. The values found in this study rise to approximately 9×10^{-11}; however, Wiebe's data show a rise to 28×10^{-11}, with a minimum of roughly 16×10^{-11}. The data by Straiton and Tolbert (ref. 5) show a similar strong increase in ϵ' as water is added.

A partial explanation of this behavior can be attributed to the variation of the dielectric constant of water with frequency (ref. 12, fig. 11.7). The real part of ϵ decreases by a factor of ~2 when the frequency is changed from 9 to 37 GHz; the imaginary part ϵ'', on the other hand, changes relatively little in the same range. The latter behavior seems to be reflected in the data for ϵ''. Values found in this study for 30 percent moisture content are in the neighborhood of 6×10^{-11}; Wiebe's values are approximately 8×10^{-11}.

Results of this study for ϵ' and ϵ'' for soil samples of loamy find sand (sample designation M5), fine sandy loam (L3), and sandy clay loam (F2) are plotted as functions of percent water by dry soil weight in figures 6 to 8.

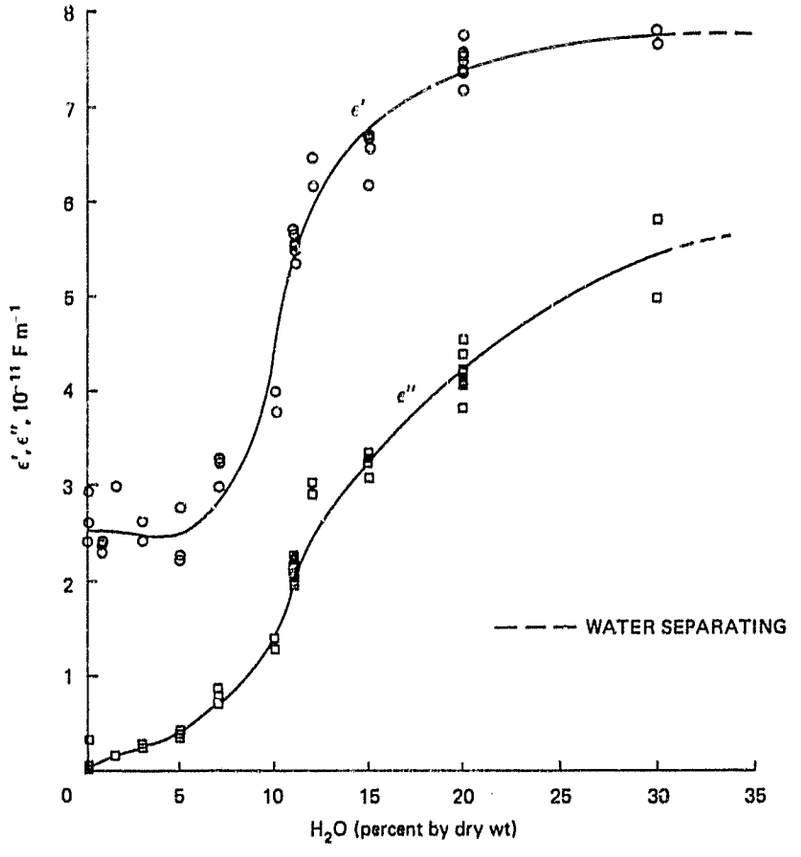

Figure 6.—Values of ϵ' and ϵ'' versus water content. Loamy fine sand sample M5, 37 GHz.

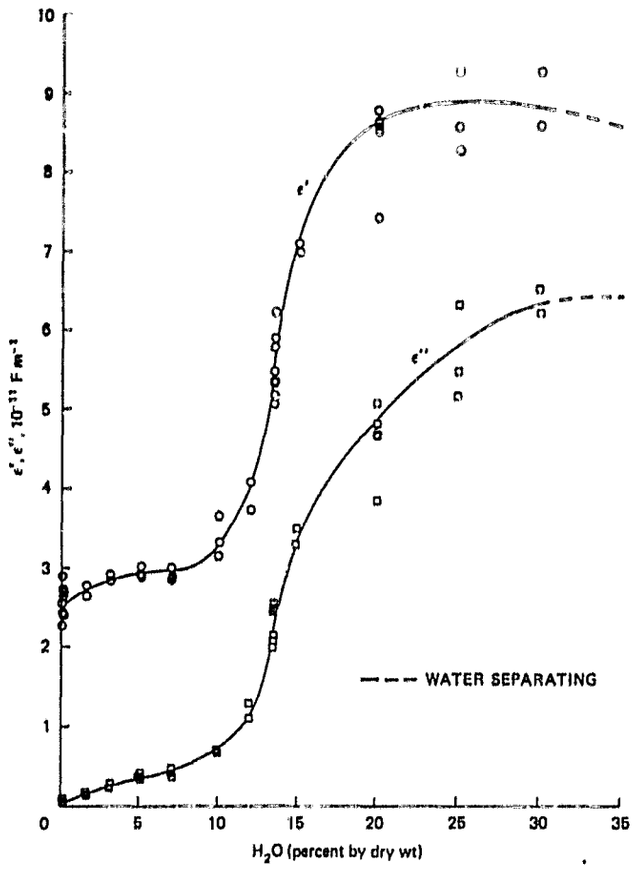

Figure 7.—Values of ϵ' and ϵ'' versus water content. Sandy clay loam sample F2, 37 GHz.

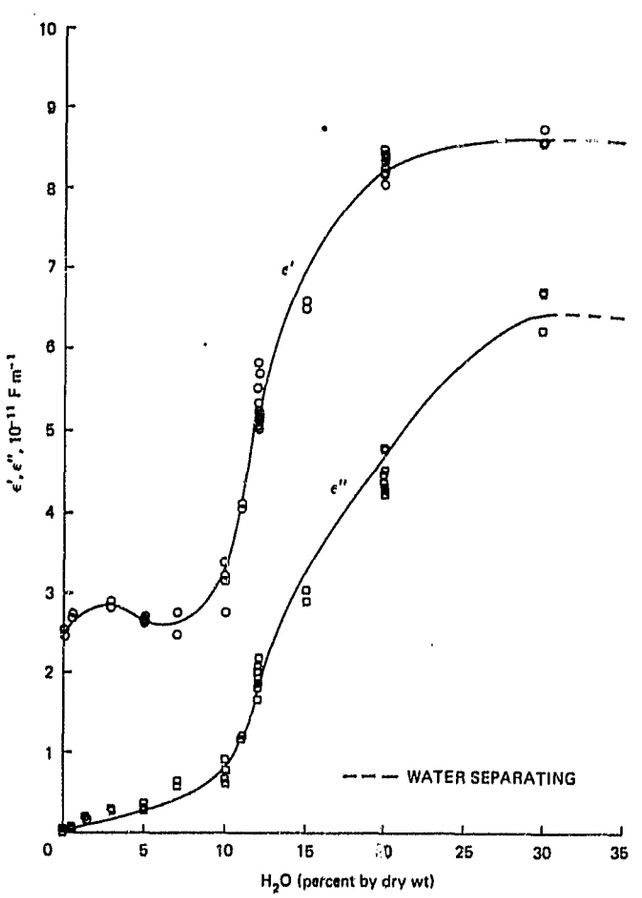

Figure 8.—Values of ϵ' and ϵ'' versus water content. Fine sandy loam sample L3, 37 GHz.

Table 3.—Textural Analysis of Phoenix, Ariz., Area Soils

Sample designation	Soil texture	Percentage composition, dry		
		Sand	Silt	Clay
M5	Loamy fine sand	88.0	7.3	4.7
L3	Fine sandy loam	48.0	34.0	18.0
F2	Sandy clay loam	56.0	26.7	17.3

Origin of the samples and their textural analysis are given in table 3. All dielectric constant determinations are shown independently on the graphs and no averages are taken. The reason for this is simply to exhibit the scatter of the results caused by differences in sample packing and sample variability. Measurements at approximately 0.6 percent water correspond to "as found" soil samples.

The most interesting and unexpected feature of the curves of ϵ' versus percent water is the behavior of ϵ' at relatively low moisture content (up to approximately 10 percent). Considering the extremely high dielectric constant of water, an immediate and substantial increase in the dielectric constant of the mixture was expected as water was added to the soil. This expectation was also based on the published data (refs. 5 and 21). But the dielectric constant observed was almost independent of or decreasing with moisture content, reaching a broad minimum in the neighborhood of 6 percent.

Further increase in water content resulted in a steep increase of ϵ'. The minimum seems to be preceded by a broad maximum—however, the data are not good enough to demonstrate this clearly. A similar drop in ϵ' is evident in data published by von Hippel (ref. 20) and Edgerton (ref. 22). However, Wiebe's data (ref. 21) show a smooth increase of ϵ' with water content; that trend may have been the result of the sample packing method (a controlled impact hammer) and the lack of detailed data in the 0- to 10-percent moisture range.

On the whole, the results for three soil samples show good agreement. The maximum dielectric constant ϵ' falls in the range from 8 to 9 $\times 10^{-11}$ F m^{-1} and ϵ'' from 5.5 to 7 $\times 10^{-11}$ F m^{-1}. The initial variation of ϵ' with moisture is relatively small, about ±30 percent, but above 10 percent water, ϵ' increases at the rate of about 1 $\times 10^{-11}$ F m^{-1} per percent of water. This extremely rapid increase of ϵ' and ϵ'' with moisture is not reflected in the free-space reflection coefficient; as a result, the microwave brightness temperature (eq. (1)) variation with water content still has manageable proportions. In fact, one can easily derive an expression for the change in brightness temperature as a function of moisture. The details of the calculation are given in appendix B.

If the soil sample has a dielectric constant $\epsilon = \epsilon' - j\epsilon''$, then the free-space amplitude reflection coefficient for normal incidence is

$$R = \frac{1 - de^{j\varphi}}{1 + de^{j\varphi}} \tag{39}$$

where

$$de^{j\varphi} = \sqrt{\frac{\epsilon'}{\epsilon_0} - \frac{j\epsilon''}{\epsilon_0}}$$

The power reflection coefficient RR^* becomes

$$RR^* = \frac{1 - 2d\cos\varphi + d^2}{1 + 2d\cos\varphi + d^2} \tag{40}$$

but $\cos\varphi \sim 1$, and

$$RR^* = \left(\frac{1-d}{1+d}\right)^2 \tag{41}$$

Calculating the total differential of RR^*, and assuming $\partial(RR^*)/\partial\varphi \sim 0$, one finds

$$\frac{d(RR^*)}{dx} = +\frac{2(d^2-1)}{\epsilon_0^2 d^3 (d+1)^4}\left(\epsilon'\frac{d\epsilon'}{dx} + \epsilon''\frac{d\epsilon''}{dx}\right) \tag{42}$$

where x is the percentage moisture. Because the radiometric brightness temperature is given by $T_b \cong (1 - RR^*)T_{soil}$, the result is

$$\frac{dT_b}{dx} = -\frac{d(RR^*)}{dx}T_{soil} \tag{43}$$

For sandy clay loam (sample F2) with 13 percent water, $\epsilon'/\epsilon_0 \sim 5$, $\epsilon''/\epsilon_0 \sim 1.5$ (from fig. 7), and

$$\frac{d(RR^*)}{dx} = 0.03\frac{d\epsilon'}{dx} + 0.01\frac{d\epsilon''}{dx}$$

From equation (43)

$$\frac{dT_b}{dx} \cong -12 \qquad \text{K/percent moisture}$$

for

$$\frac{d\epsilon'}{dx} \cong \frac{d\epsilon''}{dx} \cong 1 \qquad \text{F m}^{-1}\text{/percent moisture}$$

CONCLUSIONS

Measurements have been made of the complex dielectric constant of three types of soil from the Phoenix, Ariz., area at 37 GHz. From 0 to 40 percent distilled water was added to the dried soils in more or less regular percentage increments. Special care was used to establish the relative insensitivity of ϵ' to water content up to 10 percent and the steep

increase in the 10- to 20-percent region. The usefulness of the dielectric data for thermal sensing would therefore be limited to approximately the 10- to 20-percent moisture region. In that region the microwave brightness temperature change per percent moisture change in the soil is approximately −12 K per percent change.

All measurements were corrected for reflections at the sample interfaces. These corrections primarily affect the values of α and ϵ'' at a moisture content of up to 10 percent. For high-loss samples, corrections must be applied to both α and β. The error in α at 10 percent water content is approximately 5 percent, and at 30 percent water content, 9 percent in α and 3 percent in β. Graphs were drawn to allow the corrections $\Delta\alpha/\alpha$ and $\Delta\beta/\beta$ to be estimated for a given reflection coefficient and length of sample. Actual calculation of α, β, ϵ', and ϵ'' was done by machine iteration of transcendental equation (35). Two experimental methods were evolved to deal with lossy samples. Low-loss sample phase shifts were determined from a conveniently small section of the sample cell; when losses exceeded about 50 dB cm^{-1}, phase shifts were measured directly for the total length of the cell. Accordingly, two different computer programs were used in the calculation of the dielectric constants.

Limit expressions were derived for the proper experimental determination of β_e, the suppression of interference effects, and the convergence of the iteration calculation.

Although reflection errors can (see analysis in section entitled "Reflection Errors") be reduced to zero if the sample cell is long enough (i.e., if $\Delta\alpha L$ is constant and $\Delta\alpha \to 0$ as $L \to \alpha$); however, this is not a practical approach. The limited microwave power and sensitivity of the detection equipment limit the total amount of attenuation that can still be detected long before $\Delta\alpha$ and $\Delta\beta \to 0$. (See discussion in section entitled "Experimental Method.")

ACKNOWLEDGMENTS

The authors are indebted to Dr. P. Gloersen, Dr. T. Wilheit, and Dr. T. Schmugge for helpful discussions and suggestions.

Appendix A

PROOF OF CONVERGENCE OF ITERATION

Equation (28) can be rewritten in the form

$$[1 - R^2(\alpha, \beta)]\, e^{-\alpha L}\, e^{j\Phi} = e^{j\beta L}\, e^{-\alpha L} \tag{A-1}$$

For a given measurement, the expression on the right of the equal sign is a constant. In the iteration calculation both α and Φ are iterated, but the change of Φ with R is small, as discussed in the section entitled "Reflection Errors." Assume for the sake of simplicity that Φ is constant. Then equation (A-1) can be rewritten in the general functional form

$$f(\alpha)F(\alpha) = F(\alpha_0) \tag{A-2}$$

where

$$f(\alpha) = 1 - R^2(\alpha)$$

$$F(\alpha) = e^{-\alpha L}\, e^{j\Phi}$$

and α_0 is the experimentally obtained data and represents the first approximation to α. The term $F(\alpha_0)$ is a constant.

Write the iteration equation in the form

$$f(\alpha_r)F(\alpha_{r+1}) = F(\alpha_0) \tag{A-3}$$

and let

$$\alpha = \alpha_r + \delta\alpha_r$$

Expanding both $f(\alpha_r)$ and $F(\alpha_{r+1})$ by Taylor's theorem and using $f(\alpha)F(\alpha) = F(\alpha_0)$ gives

$$\delta\alpha_{r+1} = -\frac{\partial f/\partial\alpha}{\partial F/\partial\alpha}\,\frac{F(\alpha)}{f(\alpha)} \tag{A-4}$$

Let $\alpha_0 - \alpha_1 = \delta\alpha_0$, then

$$\delta\alpha_{r+1} = \left(-\frac{\partial f/\partial\alpha}{\partial F/\partial\alpha}\,\frac{F(\alpha)}{f(\alpha)}\right)^{r+1}\delta\alpha_0 \tag{A-5}$$

or

$$\delta\alpha_{r+1} \to 0$$

if

$$\left|\frac{f'}{F'}\frac{F}{f}\right| < 1$$

From equation (A-2), it is seen that

$$\left|\frac{f'}{F'}\frac{F}{f}\right| = \left|\frac{2R}{L}\frac{\partial R}{\partial \alpha}\right| \tag{A-6}$$

One can write

$$R = R[Z_2(\alpha)]$$

$$\frac{\partial R}{\partial \alpha} = \frac{\partial R}{\partial Z_2}\frac{\partial Z_2}{\partial \alpha} \tag{A-7}$$

Then

$$\frac{\partial R}{\partial Z} = \frac{2Z_0}{(Z_2 + Z_0)^2} \tag{A-8}$$

and from

$$Z_2 \cong \frac{\mu_0 \omega \beta}{\alpha^2 + \beta^2} \tag{A-9}$$

(the imaginary part can be neglected)

$$\frac{\partial Z_2}{\partial \alpha} \cong -\frac{2\mu_0 \omega \alpha}{\beta^3} \tag{A-10}$$

$$\frac{\partial R}{\partial \alpha} \cong -\frac{4\mu_0 \omega \alpha Z_0}{(Z_2 + Z_0)^2 \beta^3} \tag{A-11}$$

With

$\alpha \sim 200$ Np m^{-1}

$\beta \sim 2000$ rad m^{-1}

$\omega\mu_0 \sim 29 \times 10^4$

$Z_0 \sim 460\ \Omega$

$Z_2 \sim 200\ \Omega$

the result is

$$\frac{\partial R^*}{\partial \alpha} \cong 10^{-5}$$

Appendix B

CHANGE OF BRIGHTNESS TEMPERATURE WITH MOISTURE

The propagation constant for a transverse electromagnetic (TEM) wave (ref. 12, eq. (16)) is given by

$$\gamma = \sqrt{j\omega\mu(\sigma + j\omega\epsilon)} \tag{B-1}$$

Make the substitution

$$\epsilon = \epsilon' - j\epsilon''$$

and let $\sigma = 0$, then

$$\gamma = \sqrt{j\omega\mu(\omega\epsilon'' + j\omega\epsilon')} \tag{B-2}$$

Comparison with equation (B-1) shows that one can make the formal substitution $\sigma = \omega\epsilon''$.

The free wave impedance of a medium is defined (ref. 12, eq. (17)) by

$$Z = \sqrt{\frac{j\omega\mu}{\sigma + j\omega\epsilon}} \tag{B-3}$$

From the above it follows that for a lossy medium of $\epsilon = \epsilon' - j\epsilon''$,

$$Z = \sqrt{\frac{j\mu}{\epsilon'' + j\epsilon'}} \tag{B-4}$$

The amplitude reflection coefficient for normal incidence for the E vector of a TEM wave incident on a medium of wave impedance Z_2 (ref. 17) is

$$R_E = \frac{Z_2 - Z_0}{Z_2 + Z_0} \tag{B-5}$$

Substitution for Z_2 and $Z_0 = \sqrt{\mu_0/\epsilon_0}$ gives

$$R_E = \frac{1 - \sqrt{\epsilon'/\epsilon_0 - j\epsilon''/\epsilon_0}}{1 + \sqrt{\epsilon'/\epsilon_0 - j\epsilon''/\epsilon_0}} \tag{B-6}$$

Let

$$\sqrt{\frac{\epsilon'}{\epsilon_0} - \frac{j\epsilon''}{\epsilon_0}} = de^{j\varphi}$$

then

$$\cos 2\varphi = \frac{\epsilon'/\epsilon_0}{\sqrt{(\epsilon'/\epsilon_0)^2 + (\epsilon''/\epsilon_0)^2}}$$

$$d = \left[\left(\frac{\epsilon'}{\epsilon_0}\right)^2 + \left(\frac{\epsilon''}{\epsilon_0}\right)^2\right]^{1/4}$$

And one can write

$$R_E = \frac{1 - de^{j\varphi}}{1 + de^{j\varphi}} \tag{B-7}$$

The power reflection coefficient then becomes

$$R_E R_E^* = \left(\frac{1 - d}{1 + d}\right)^2 \tag{B-8}$$

Because $\epsilon' > \epsilon''$, $\cos 2\varphi \sim 1$, and $\cos\varphi \sim 1$. The total differential of RR^* is calculated from the partial differentials, $\partial R/\partial d$, $\partial d/\partial \epsilon'$, and $\partial d/\partial \epsilon''$, resulting in

$$d(R_E R_E^*) = -\frac{2(d^2 - 1)}{\epsilon_0^2 (1 + d)^4 d^3} (\epsilon'\, d\epsilon' + \epsilon''\, d\epsilon'') \tag{B-9}$$

REFERENCES

1. Staelin, D. H.: "Passive Remote Sensing at Microwave Wavelengths." *Proc. IEEE* 57: 427, 1969.

2. Kurskaya, A. A.; Fedorova, L. V.; and Yakovleva, G. D.: *Transfer of Microwave Radiation in the Atmosphere.* K. S. Shifrin, ed., NASA TT F-590, 1969, p. 56.

3. Westphal, W. B.: "Techniques of Measuring the Permittivity and Permeability of Liquids and Solids in the Frequency Range 3 c/s to 50 KMc/s." Report LIR-36, Laboratory for Insulation Research, MIT, July 1950, p. 46.

4. Buchanan, T. J.: "Balance Methods for the Measurement of Permittivity in the Microwave Region." *Proc. Inst. Elec. Eng.* 99: 61, 1952.

5. Straiton, A. W.; and Tolbert, C. W.: "Measurement of the Dielectric Properties of Soils and Water at 3.2 cm Wave Length." *J. Franklin Inst.* 246: 13, 1948.

6. Cumming, W. A.: "The Dielectric Properties of Ice and Snow at 3.2 Centimeters." *J. Appl. Phys.* 23: 768, 1952.

7. Roberts, S.; and von Hippel, A.: "A New Method for Measuring Dielectric Constant and Loss in the Range of Centimeter Waves." *J. Appl. Phys.* 17: 610, 1946.

8. Horner, F.; Tayler, T. A.; Dunsmuir, R.; Lamb, J.; and Jackson, Willis: "Resonance Methods of Dielectric Measurement at Centimeter Wavelengths." *J. Inst. Elec. Eng.* Part 3, 93: 53, 1946.

9. Tkach, V. K.; Stepin, L. D.; and Kazarskii, V. B.: "Resonance Method of Measuring the Dielectric Permittivity and the Tangent of the Loss Angle of Liquid Dielectrics." *Radio Eng. Electron. Phys.* 5(12): 200, 1960. (Translated from Russian.)

10. Hertel, P.; Straiton, A. W.; and Tolbert, C. W.: "Dielectric Constant Measurements at 8.6 mm Wavelength." *J. Appl. Phys.* 24: 956, 1953.

11. Pozdniak, S. I.: "Measurement of the Electrical Properties of a Medium by a Polarization Method." *Radio Eng. Electron. Phys.* 5(10): 271, 1960. (Translated from Russian.)

12. Dicke, R. H.; and Purcell, E. M.: *Principles of Microwave Circuits,* C. G. Montgomery, ed., MIT Rad. Lab. Series, vol. 8, 1948.

13. Born, M.: *Optik.* Springer Verlag (Berlin), 1933, sec. 39.

14. Stratton, J. A.: *Electromagnetic Theory.* McGraw-Hill Book Co., Inc., 1941, sec. 9.10.

15. Goubau, G.: *Electromagnetic Waveguides and Cavities.* Pergamon Press, 1961, ch. IV, eq. (13.1).

16. Altman, J.: *Microwave Circuits.* D. Van Nostrand Co., Inc., 1964, sec. 2.5.

17. Schelkunoff, S. A.: *Electromagnetic Waves.* D. Van Nostrand Co., Inc., 1943, ch. 8, sec. 8.4.

18. Smith-Rose, R. L.: "The Electrical Properties of Soil for Alternating Currents at Radio Frequencies." *Proc. Roy. Soc. Ser. A* 140: 359, 1933.

19. Ford, L. H.; and Oliver, R.: "An Experimental Investigation of the Reflection and Absorption of Radiation of 9 cm Wavelength." *Proc. Phys. Soc. London* 58: 265, 1946.

20. Hippel, A. von, ed.: *Dielectric Materials and Applications.* John Wiley & Sons, Inc., 1961, p. 314.

21. Wiebe, M. L.: "Laboratory Measurement of the Complex Dielectric Constant of Soils." Tech. Rept. RSC-23 (NASA Grant NsG 239-62), Texas A&M Univ., College Station, Tex., Oct. 1971.

22. Edgerton, A. T.: "Determination of Soil Moisture Content Using Microwave Radiometry." Tech. Rept. 1684 FR-1, Aerojet-General Corp., El Monte, Calif., 1971.